physica status solidi a
www.pss-a.com
applications and materials science

Interpretation of capacitance spectra and transit times of single carrier space-charge limited transport in organic layers with field-dependent mobility

José M. Montero[1], **Juan Bisquert**[1], **Germà Garcia-Belmonte**[1], **Henk J. Bolink**[2], and **Eva M. Barea**[1]

[1] Departament de Física, Universitat Jaume I, 12071 Castelló, Spain
[2] Institut de Ciència Molecular, Universitat de València, Polígon La Coma s/n, 46980 Paterna, València, Spain

Received 20 January 2007, revised 13 March 2007, accepted 16 March 2007
Published online 15 May 2007

PACS 72.10.Bg, 72.20.Ht, 72.80.Le, 73.61.Ph

The ac impedance characteristics of a single carrier with space-charge limited current (SCLC) transport in organic layers with field-dependent mobility is analyzed, indicating the similarities as well as the differences to the constant mobility case. The model provides capacitance spectra and transit times from different calculation methods, in relation to the electric field distribution in the SCLC regime. It is found that the low frequency capacitance lies in the range $3C_g/4 < C_{lf} < C_g$, with respect to the geometric capacitance C_g. An approximated expression for the variation of the transit time with applied bias is derived, in good agreement with exact calculations. Experimental results of capacitance spectra of hole-only PPV devices indicate the validity of the SCLC model but also show a strong contribution of trapping at low frequencies that overlap the low-frequency value of the SCLC capacitance.

phys. stat. sol. (a) **204**, No. 7, 2402–2410 (2007) / **DOI** 10.1002/pssa.200723028

physica status solidi a

phys. stat. sol. (a) **204**, No. 7, 2402–2410 (2007) / **DOI** 10.1002/pssa.200723028

Interpretation of capacitance spectra and transit times of single carrier space-charge limited transport in organic layers with field-dependent mobility

José M. Montero[1], **Juan Bisquert**[*, 1], **Germà Garcia-Belmonte**[1], **Henk J. Bolink**[2], and **Eva M. Barea**[1]

[1] Departament de Física, Universitat Jaume I, 12071 Castelló, Spain
[2] Institut de Ciència Molecular, Universitat de València, Polígon La Coma s/n, 46980 Paterna, València, Spain

Received 20 January 2007, revised 13 March 2007, accepted 16 March 2007
Published online 15 May 2007

PACS 72.10.Bg, 72.20.Ht, 72.80.Le, 73.61.Ph

The ac impedance characteristics of a single carrier with space-charge limited current (SCLC) transport in organic layers with field-dependent mobility is analyzed, indicating the similarities as well as the differences to the constant mobility case. The model provides capacitance spectra and transit times from different calculation methods, in relation to the electric field distribution in the SCLC regime. It is found that the low frequency capacitance lies in the range $3C_g/4 < C_{lf} < C_g$, with respect to the geometric capacitance C_g. An approximated expression for the variation of the transit time with applied bias is derived, in good agreement with exact calculations. Experimental results of capacitance spectra of hole-only PPV devices indicate the validity of the SCLC model but also show a strong contribution of trapping at low frequencies that overlap the low-frequency value of the SCLC capacitance.

1 Introduction

Organic materials are being investigated to develop modern optoelectronic devices such as organic field effect transistors, organic solar cells and organic light emitting diodes (OLEDs) by simple spin-coating techniques. In these devices the charge injection and transport determines to a large extend their performances. If carriers can easily overcome energy barriers at the interfaces (anode and cathode), the current should be bulk-limited and not injection-limited. In this situation, the ohmic regime has a narrow initial dominium (milivolts) whereas space-charge limited current (SCLC) regime dominates widely the charge transport within the organic layer. In a dual carrier device (in which both holes and electrons are injected) it is complicated to derive independent transport parameters for the separate electronic carriers. To overcome this hurdle hole-only devices can be prepared by using a high workfunction cathode that prevents the injection of electrons. These devices exhibit an unipolar current that is SCL as well.

SCLC regime is often observed in the current density–potential (J–V) characteristics of polymer light emitting diodes (PLEDs). The ac impedance measurement has the advantage that it provides additional information, i.e. capacitance and transit time, with respect to dc methods, and some authors have applied these methods to obtain parameters governing single carrier transport in organic layers [1–5]. These works apply the standard SCLC impedance model that is valid for constant mobility [6, 7], in some cases extended with a dispersive (frequency-dependent) mobility [1, 2] and for bipolar devices [1, 3–5, 8].

* Corresponding author: e-mail: bisquert@uji.es

It is well established that in organic layers the mobility depends on the local electrical field E as [9–13]

$$\mu(E) = \mu_0 \exp\left(\gamma\sqrt{E}\right), \tag{1}$$

where μ_0 denotes the mobility of electrons or holes at zero field and γ is the parameter describing the field dependence [14]. Many studies have shown that Eq. (1) produces a dramatic change of the dependence of steady-state current–potential characteristics. It is therefore likely that the field-dependent mobility introduces significant changes in the ac impedance model of SCLC. To our knowledge, only Berleb and Brütting have considered this effect [2], but their study is not completely correct, because they fail to include the modulation of the field in the expression of the mobility, see Eq. (12), below. Here we provide the solution to this problem and discuss the characteristics of ac impedance of a single carrier in SCLC, with a view to the interpretation of capacitances and transit times in PLEDs and other organic electronic devices. Steady-state and capacitance measurements of hole-only devices are discussed as well, to check the application of the model. A recent study by Coehoorn et al. [15] takes all the relevant aspects into account, however they consider a density-dependent mobility, with an exponential distribution of traps, and they are able to produce an analytic solution for the impedance. Their study and ours may be regarded as complementary, covering the most important expressions generally used to describe variations of the mobility in organic layers.

2 Theory

2.1 AC Impedance and capacitance spectra

The SCLC for unipolar transport (neglecting diffusion) is described by the continuity equation, the drift and displacement current equation and the Poisson equation, respectively:

$$\frac{\mathrm{d}J}{\mathrm{d}x} = 0\,, \tag{2}$$

$$J = p(x)\, e\mu[E(x)]\, E(x) + \varepsilon \frac{\partial E(x)}{\partial t}\,, \tag{3}$$

$$\frac{\varepsilon}{e}\frac{\mathrm{d}E(x)}{\mathrm{d}x} = p(x)\,, \tag{4}$$

where $p(x)$ is the carrier density at position x, $\varepsilon = \varepsilon_0\varepsilon_\mathrm{r}$ the permittivity of the polymer, and e the positive elementary charge. The collecting contact is at $x = L$. The electric potential relates to the electric field as

$$V = \int_0^L E\,\mathrm{d}x\,. \tag{5}$$

The impedance is defined as the quotient of potential to current density

$$Z(\omega) = \hat{V}(\omega)/\hat{j}(\omega)\,, \tag{6}$$

where the tilde denotes a small ac perturbation of angular frequency ω over a steady-state. The frequency-dependent capacitance is defined as

$$C'(\omega) = \mathrm{Re}\,[1/i\omega Z(\omega)]\,. \tag{7}$$

The impedance model for SCLC with a constant mobility is well known [6, 7] and it has the expression

$$Z(\omega) = \frac{6}{g_0(i\omega\tau_\mathrm{tr})^3}\left[1 - i\omega\tau_\mathrm{tr} + \frac{1}{2}(i\omega\tau_\mathrm{tr})^2 - \mathrm{e}^{-i\omega\tau_\mathrm{tr}}\right], \tag{8}$$

where

$$\tau_{\mathrm{tr}} = \frac{4}{3}\frac{L^2}{\mu V_{\mathrm{dc}}}, \tag{9}$$

$$g_0 = \frac{9}{4}\varepsilon\mu_0\frac{V_{\mathrm{dc}}}{L^3} = \frac{\mathrm{d}j_{\mathrm{dc}}}{\mathrm{d}V_{\mathrm{dc}}}, \tag{10}$$

$$C_{\mathrm{g}} = \frac{\varepsilon}{L}, \tag{11}$$

are the transit time, dc conductance and geometrical capacitance, respectively. The capacitance obtained from Eq. (7) takes the value of the geometric capacitance C_{g} at high frequencies, and at the frequency of the transit time, τ_{tr}, decreases to $3C_{\mathrm{g}}/4$ towards low frequencies.

Let us consider the ac impedance model of SCLC for a single carrier with field-dependent mobility as stated in Eq. (1). It is formulated separating the stationary components from the small perturbation ac parts in the drift equation. The mobility dependence on the field implies, up to first order, the following expression

$$\mu(E_{\mathrm{dc}} + \hat{E}) = \mu(E_{\mathrm{dc}}) + \frac{\partial\mu}{\partial E}\hat{E}. \tag{12}$$

Therefore we obtain the equation

$$J_{\mathrm{dc}} + \hat{j} = e[p_{\mathrm{dc}} + \hat{p}]\left[\mu(E_{\mathrm{dc}}) + \frac{\partial\mu}{\partial E}\hat{E}\right]\left[E_{\mathrm{dc}} + \hat{E}\right] + i\omega\varepsilon\hat{E}. \tag{13}$$

The zero order gives the steady state equation

$$J_{\mathrm{dc}} = p_{\mathrm{dc}} e\mu(E_{\mathrm{dc}})\, E_{\mathrm{dc}}. \tag{14}$$

In combination with Eq. (1), the $J(V)$ dependence from this last equation has been recently solved in a parametric form [16, 17] and corroborates the very accurate explicit approximation of Murgatroyd [18]:

$$J = \frac{9}{8}\frac{\varepsilon\mu_0}{L^3}V^2\, \mathrm{e}^{0.89\gamma\sqrt{V/L}}. \tag{15}$$

The small signal terms in Eq. (13), in combination with Poisson's equation, provide the equation

$$\hat{j} = ep_{\mathrm{dc}}\mu'(E_{\mathrm{dc}})\,\hat{E} + \varepsilon\mu(E_{\mathrm{dc}})\,E_{\mathrm{dc}}\frac{\partial\hat{E}}{\partial x} + i\omega\varepsilon\hat{E}, \tag{16}$$

where

$$\begin{aligned}\mu'(E_{\mathrm{dc}}) &= \mu + \frac{\partial\mu}{\partial E}E_{\mathrm{dc}} \\ &= \mu_0\left[1 + \frac{\gamma}{2}\sqrt{E_{\mathrm{dc}}}\right]\exp\left(\gamma\sqrt{E_{\mathrm{dc}}}\right).\end{aligned} \tag{17}$$

The impedance is obtained from the solution of Eq. (16) with respect to $\hat{V}$, which is obtained numerically. Figure 1 shows capacitance spectra at different bias potentials. In contrast to the constant mobility case, the shape of the spectra depend on the stationary operation point. The transition from low (C_{lf}) to high frequency (C_{g}) value is displaced to higher frequency at higher bias potential, indicating a reduction of the transit time. In addition, the low frequency capacitance increases with applied bias and its values

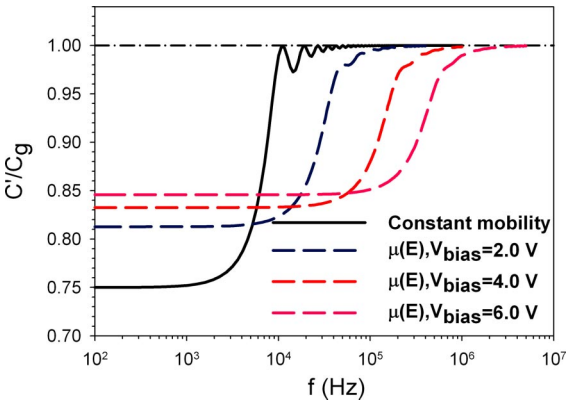

Fig. 1 (online colour at: www.pss-a.com) Simulations of capacitance spectra of a single carrier injected into an organic layer of thickness $L = 125$ nm with parameters $\mu_0 = 4.6\times10^{-7}$ cm^2/Vs, $\gamma = 5.4\times10^{-3}(cm/V)^{1/2}$, $\varepsilon_r = 3$ and for different applied bias.

are higher than $3C_g/4$. For the high frequency regime, capacitance amounts to C_g as in the constant mobility case. In an early study [19], the values of low frequency capacitance are found to be sensitive to the specific dependence of mobility on the local field, although the characteristic formula Eq. (1) for organic conductors was not described at that time. The origin of the low frequency capacitance being lower than C_g is discussed by Kassing [20] in terms of three contributions to the capacitance that arise in Eq. (16): velocity modulation, density modulation, and a displacement term, respectively. It is noteworthy that in the study of Coehoorn et al. [15] with density-dependent mobility, the low frequency capacitance is lower than the constant mobility case value, i.e., $C_{lf} < 3C_g/4$, while for Eq. (1), we have remaked that it is always $3C_g/4 < C_{lf} < C_g$.

2.2 Transit times

The dc transit time is obtained integrating the reciprocal of the drift velocity as:

$$\tau_{trdc} = \int_0^L \frac{1}{\mu(E)\,E}\,\mathrm{d}x\,. \tag{18}$$

A lower transit time is expected with respect to the constant mobility case because carriers drift velocity is increased with the exponential dependence of the mobility on the field.

Figure 2 shows the electric field distribution for a given bias potential in different cases:

– $\gamma = 0$ describes the constant mobility electric field distribution.

– $\gamma = \gamma_0$ describes the field-dependent mobility electric field distribution for characteristic γ values.

– $\gamma = 6\times\gamma_0$ describes the field-dependent mobility electric field distribution for extreme γ values.

As shown in Fig. 2, when the mobility increases rapidly with the field, the field increases more slowly towards the extracting contact. Since carriers mobility is increased by their field-dependence, more of them can penetrate in the material and establish a larger carrier distribution with regard to the constant mobility case. In order to maintain a constant current, Eq. (2), the system reacts decreasing the electric field. This causes the electric field distribution with a stronger field-dependent mobility to approach a uniform electrical field. Therefore, we can apply the following approximations in order to obtain a simplified expression for the transit time. Assuming

$$\sqrt{E(x)} \approx \sqrt{V/L}\,, \tag{19}$$

Eq. (1) becomes a field-independent mobility with a correcting exponential factor,

$$\mu(E) \approx \mu_0 \exp\left(\gamma\sqrt{V/L}\right). \tag{20}$$

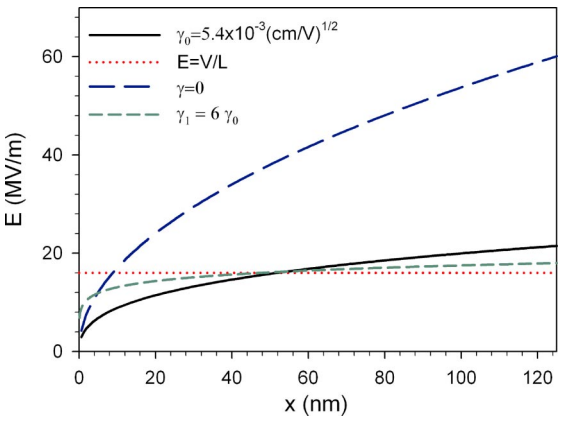

Fig. 2 (online colour at: www.pss-a.com) Distribution of electric field for single carrier injected into an organic layer of thickness $L = 125$ nm with a bias voltage 2.0 V, with parameters $\mu_0 = 4.6 \times 10^{-7}$ cm^2/Vs, $\varepsilon_r = 3$ and various values of γ as indicated. An approximation to the ohmic regime is also shown.

Finding the stationary solution for the system of Eqs. (2)–(4) with Eq. (20), we obtain the well known Child's law and electric field distribution in space with the corrected constant mobility by using the same derivation as for constant mobility [21]

$$J \approx \frac{9}{8} \varepsilon \mu_0 \exp\left[\gamma \sqrt{V/L}\right] \frac{V^2}{L^3}, \tag{21}$$

$$E(x) \approx \left(\frac{2Jx}{\varepsilon \mu_0 \exp\left[\gamma \sqrt{V/L}\right]} \right)^{1/2}. \tag{22}$$

Replacing the current, Eq. (21), in Eq. (22), we obtain

$$E(x) \approx \frac{3}{2} \frac{V}{L^{3/2}} \sqrt{x}. \tag{23}$$

Substituting Eqs. (20) and (23) in Eq. (18) and integrating, we arrive at

$$\tau_{\mathrm{dctr}} \approx \frac{4}{3} \frac{L^2}{\mu_0 \exp\left[\gamma \sqrt{V/L}\right] V}, \tag{24}$$

which is simply the classical expression for transit times with constant mobility, Eq. (9), including an exponential dependence due to field-dependent mobility.

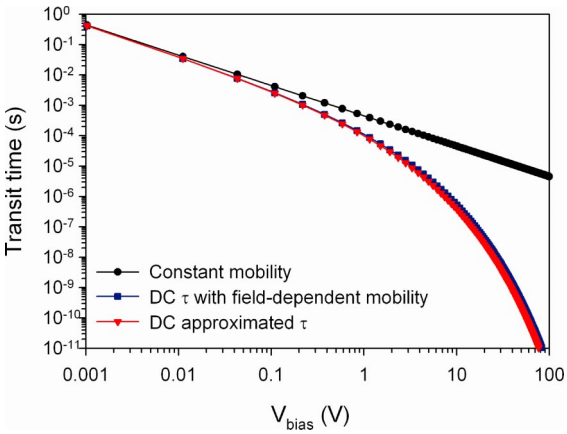

Fig. 3 (online colour at: www.pss-a.com) Transit times of a single carrier in an organic layer with different integrated expressions described in the main text. Deviation from the constant mobility case is shown.

In Fig. 3 the dc-transit times have been represented using different formulas: Constant mobility transit time, Eq. (9); the field-dependent mobility transit time, Eq. (18), and the approximated expression of field-dependent transit time, Eq. (24). The results in Fig. 3 show that the dc transit time with a field-dependent mobility departs strongly from the constant mobility transit time. In addition it is observed that Eq. (24) gives an excellent approximation to the exact dc transit time in Eq. (18).

As mentioned above, the time needed for carriers to cross the device thickness can also be obtained from the frequency of change of capacitance spectrum in the transition form high to low frequency values. For low frequencies, ac-carriers injected have enough time to reach the opposite electrode under the influence of background dc electric field and the capacitance has a low value. Increasing the voltage modulation, ac-carriers can not keep up with the signal at a critical frequency that marks the capacitance step. A common method to define an ac-transit time consists in analyzing the change of susceptance $-\Delta B = -\omega(C' - C_g)$ which gives the critical frequency at the maximum of the susceptance plots [3, 4]. The ac-transit time is given approximately by

$$\tau_{\text{actr}} \approx 0.72 \cdot f_{\max}^{-1} \tag{25}$$

Figure 4 shows the calculated susceptance spectra at different bias values for characteristic mobility parameters μ_0, γ. Using Eqs. (24) and (25) we can obtain mobility values $\mu_0 \exp\left[\gamma\sqrt{V/L}\right]$ from the peak frequency and compare them with the originally postulated values. This is shown in Fig. 5. The results indicate that expressions (24) and (25) are suitable for derivation of the mobility from ac impedance data.

In order to further test the suggested approximations, rather high γ and bias-potential values $\gamma\sqrt{E} \approx 20$ are used to generate a set of transit times. These values are expected to provide a very strong departure from the field-independent mobility expressions. Figure 6 shows transit times provided by the ac method from susceptance peaks, Eq. (25), by the dc integrated expression, Eq. (18), and by the postulated approximated expression, Eq. (24). It is observed that the different methods provide similar values and the same bias-dependence of the transit time, even in this extreme case simulation, though the different values are offset by a factor 2–4.

2.3 Trapping effects

Trapping and subsequent release of charges from trap states result in an additional contribution to capacitance at low frequencies [7]. For a single trap level with a relaxation time τ_{trap} the frequency dependence of the excess capacitance is given by

$$\Delta C_t \propto \frac{1}{1 + (\omega\tau_{\text{trap}})^2}\,, \tag{26}$$

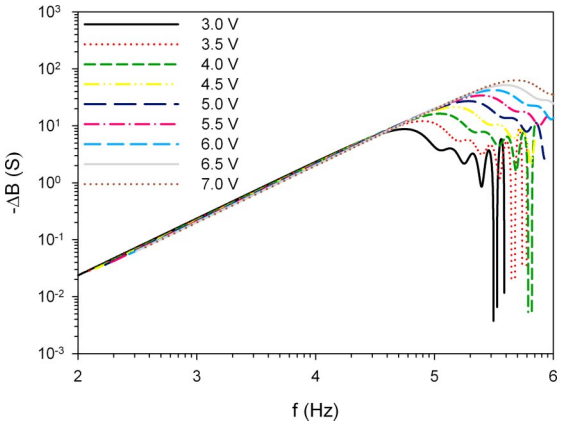

Fig. 4 (online colour at: www.pss-a.com) Susceptance spectra for a single carrier in an organic layer of thickness $L = 125$ nm, calculated numerically with parameters $\mu_0 = 4.6 \times 10^{-7}$ cm^2/Vs, $\gamma = 5.4 \times 10^{-3}$ (cm/V)$^{1/2}$, $\varepsilon_r = 3$, with different values of applied bias potential as indicated.

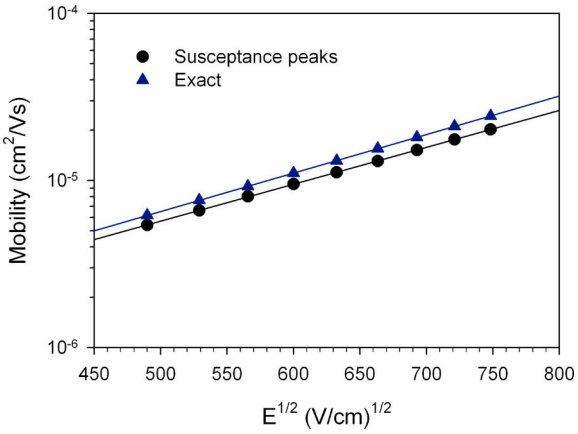

Fig. 5 (online colour at: www.pss-a.com) Mobility values obtained from susceptance peaks (linear fit gives $\mu_0 = 4.5\times10^{-7}$ cm^2/Vs, $\gamma = 5.1\times10^{-3}$ (cm/V)$^{1/2}$) compared to the initial values used in the simulation ($\mu_0 = 4.6\times10^{-7}$ cm^2/Vs, $\gamma = 5.3\times10^{-3}(cm/V)^{1/2}$).

i.e., the capacitance due to trapping increases and saturates at low frequencies ($\omega < \tau_{trap}^{-1}$). At higher frequencies the release rate from the traps can not keep up with the voltage modulation and the contribution due to trapping becomes negligible.

3 Experimental

Hole only devices of the well known polyphenylenevinylene (PPV) co-polymer "super yellow" (SY), kindly donated by Merck OLED Materials, are prepared by spincoating a filtered solution of SY in toluene on extensively cleaned and UV-Ozone treated ITO covered glass plates under cleanroom conditions in ambient atmosphere, after which they are transferred to in an inert atmosphere chamber (<0.1 ppm O_2 and <0.1 ppm H_2O) and heated for 1 hour at 80 °C. Subsequently they are transferred to a vacuum chamber integrated in a N_2 atmosphere. To remove any adsorbed moisture from the organic surface, the films were evacuated to a high vacuum of $\leq 10^{-6}$ mbarr for several hours. After this procedure Au was evaporated at high vacuum. The thickness of the SY film was determined to be 80 nm using an Ambios XP1 profilometer. Current density–potential (*J*–*V*) characteristics and impedance spectra were collected using an AutoLab PGSTAT30 equipment. An oscillating amplitude of 10 mV was added to the dc bias using frequencies within the range of 1 MHz down to 1 Hz. All measurements were performed in inert atmosphere (<0.1 ppm O_2 and <0.1 ppm H_2O).

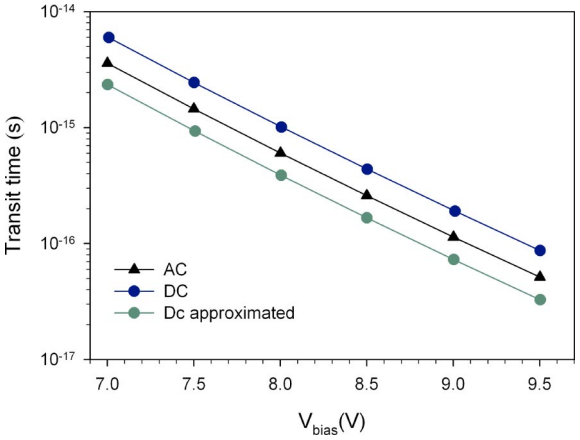

Fig. 6 (online colour at: www.pss-a.com) Transit times of a single carrier in an organic layer with extreme values of field-dependent mobility ($\gamma\sqrt{E} \approx 20$) using different calculation methods as described in the main text.

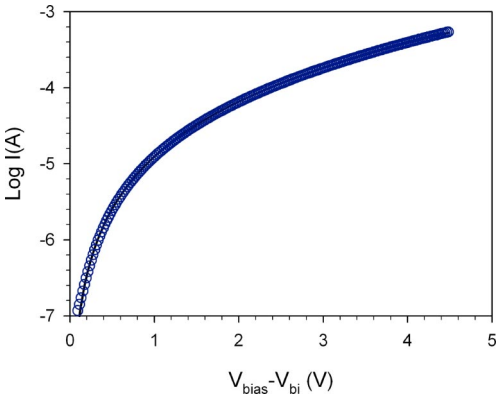

Fig. 7 (online colour at: www.pss-a.com) Experimental results (points) of current versus voltage in a hole-only device with $L = 80$ nm. The line is a fit using the formula of Murgatroyd in the SCLC regime with a built-in voltage $V_{bi} = 0.5$ V.

4 Results and discussion

A representative experimental J–V curve of a device ($L = 80$ nm, active area 9.5×10^{-2} cm^2) is shown in Fig. 7 and it is very well described by Eq. (15), indicating a field-dependent mobility. The fit of the data provides the mobility parameters ($\mu_0 = 1.73 \times 10^{-7}$ cm^2/Vs and $\gamma = 1.91 \times 10^{-3}$ (cm/V)$^{1/2}$). Using these values and extracting the permittivity ($\varepsilon_r = 2.34$) from the maximum value of the high frequency capacitance, see Eq. (11), capacitance spectra have been generated and compared with the experimental data as shown in Fig. 8. It is observed that the measured spectra display the onset of the geometric capacitance value at the frequencies predicted by the theory, which gives a confirmation of the applicability of the SCLC impedance model that has been proposed above. Two deviations are observed between experimental curves and the model proposed, which are due to additional effects that were not included in this model. On the one hand, the high frequency part of the capacitance exhibits a pronounced frequency dependence, in contrast with our assumption of a constant geometric (dielectric) capacitance. The dielectric response of disordered polymers is known to be modeled by using empirical relaxation functions [1, 22] that account for the slight decrease in the capacitance value. Such effect is then dielectric in nature and so it is not considered in our ac transport model. We have used a permittivity value corresponding to the maximum reached by the capacitance spectra in the simulation shown in Fig. 8. It has been verified that the transit frequency is not much affected by the permittivity value used around 2. On the other hand, a strong contribution of traps, is appreciated at low frequency in the experimental data. This fact prevents us from observing the low frequency value of the capacitance, which would be an interesting

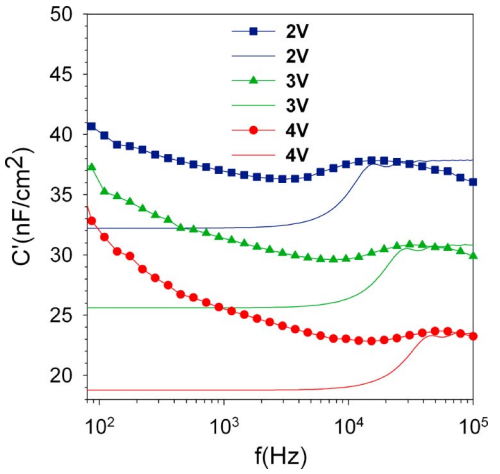

Fig. 8 (online colour at: www.pss-a.com) Experimental results of capacitance spectra at different bias potentials ranging from 2 V to 4 V (line and scatter plots) with their respective numerical calculations of the SCLC capacitance using the parameters from the fit in Fig. 7 (line plots). An offset of 6 nF cm^{-2} between every curve has been made in the picture.

additional check of the mobility dependence on electrical field as described above in the theory section. Nevertheless these results show that it is possible to evaluate the ac transit time from capacitance data as a function of the frequency.

5 Conclusions

The transit time of a single carrier in SCLC with field-dependent mobility has a lower value than in the constant mobility case, as one would expect, due to the increase of the drift velocity, and it depends strongly on the polarization. Furthermore the mobility dependence on the field tends to flatten the electrical field towards a constant value, which allows us to provide a simplified formula for the dc transit time that is in good agreement with the exact value. Experimental capacitance spectra of single carrier devices can be predicted numerically and describe well the capacitance step in the measured spectra, however the latter contain a strong contribution at low frequencies due to trapping and release of carriers and also frequency dispersion in the dielectric capacitance of the polymer.

Acknowledgements We would like to thank Dr. Spreitzer and Dr. Becker from Merck OLED materials GmbH for the donation of the super yellow. Support of Ministerio de Educación y Ciencia of Spain under project MAT2004-05168, MAT2004-03849 and Fundació Caixa Castelló-Bancaixa under project P1 1B2005-12 is acknowledged. H.B. acknowledges the support of the Program "Ramon y Cajal" of the Spanish Ministry of Education and Science.

References

[1] H. C. F. Martens, H. B. Brom, and P. W. M. Blom, Phys. Rev. B **60**, R8489 (1999).
[2] S. Berleb and W. Brütting, Phys. Rev. Lett. **89**, 286601 (2002).
[3] J. Bisquert, G. Garcia-Belmonte, A. Pitarch, and H. Bolink, Chem. Phys. Lett. **422**, 184 (2006).
[4] H. C. F. Martens, J. N. Huiberts, and P. W. M. Blom, Appl. Phys. Lett. **77**, 1852 (2000).
[5] A. Pitarch, G. Garcia-Belmonte, J. Bisquert, and H. Bolink, J. Appl. Phys. **100**, 084502 (2006).
[6] J. Shao and G. T. Wright, Solid-State Electron. **3**, 291 (1961).
[7] R. Kassing, Solid State Commun. **15**, 673 (1974).
[8] D. Poplavskyy and F. So, J. Appl. Phys. **98**, 014501 (2006).
[9] D. M. Pai, J. Phys. Chem. **52**, 2285 (1970).
[10] H. Bässler, phys. stat. sol. (b) **175**, 15 (1993).
[11] P. W. M. Blom, M. J. M. de Jong, and M. G. van Munster, Phys. Rev. B **55**, R656 (1997).
[12] P. S. Davids, I. H. Campbell, and D. L. Smith, J. Appl. Phys. **82**, 6319 (1997).
[13] B. K. Crone, P. S. Davids, I. H. Campbell, and D. L. Smith, J. Appl. Phys. **84**, 833 (1998).
[14] I. I. Fishchuk, A. Kadashchuk, H. Bässler, and M. Abkowitz, Phys. Rev. B **70**, 245212 (2004).
[15] B. Ramachandhran, H. G. A. Huizing, and R. Coehoorn, Phys. Rev. B **73**, 233306 (2006).
[16] J. Bisquert, J. M. Montero, H. Bolink, E. M. Barea, and G. Garcia-Belmonte, phys. stat. sol. (a) **203**, 3762–3767 (2006).
[17] R. H. Young, Philos. Mag. Lett. **70**, 331 (1994).
[18] P. N. Murgatroyd, J. Phys. D **3**, 151 (1970).
[19] A. Shumka and M.-A. Nicolet, Solid-State Electron. **6**, 106 (1964).
[20] R. Kassing, phys. stat. sol. (a) **28**, 107 (1975).
[21] A. van der Ziel, Solid State Physical Electronics (Prentice-Hall, Englewood Cliffs, 1976).
[22] H. H. P. Gommans, M. Kemerink, G. G. Andersson, and R. M. Tijper, Phys. Rev. B **69**, 155216 (2004).

